

Perception Reinforcement Using Auxiliary Learning Feature Fusion: A Modified Yolov8 for Head Detection

1st Jiezhou Chen

*College of Mechatronics and Control
Engineering
Shenzhen University
Shenzhen, China
chenjiezhou2022@email.szu.edu.cn*

2nd Guankun Wang

*Department of Electronic Engineering
The Chinese University of Hong Kong
Hong Kong, China
gkwang@link.cuhk.edu.hk*

3rd Weixiang Liu

*College of Mechatronics and Control
Engineering
Shenzhen University
Shenzhen, China
wxliu@szu.edu.cn*

4th Xiaopin Zhong

*College of Mechatronics and Control
Engineering
Shenzhen University
Shenzhen, China
xzhong@szu.edu.cn*

5th Yibin Tian

*College of Mechatronics and Control
Engineering
Shenzhen University
Shenzhen, China
ybtian@szu.edu.cn*

6th ZongZe Wu

*College of Mechatronics and Control
Engineering
Shenzhen University
Shenzhen, China
zzwu@szu.edu.cn*

Abstract—Head detection provides distribution information of pedestrian, which is crucial for scene statistical analysis, traffic management, and risk assessment and early warning. However, scene complexity and large-scale variation in the real world make accurate detection more difficult. Therefore, we present a modified Yolov8 which improves head detection performance through reinforcing target perception. An Auxiliary Learning Feature Fusion (ALFF) module comprised of LSTM and convolutional blocks is used as the auxiliary task to help the model perceive targets. In addition, we introduce Noise Calibration into Distribution Focal Loss to facilitate model fitting and improve the accuracy of detection. Considering the requirements of high accuracy and speed for the head detection task, our method is adapted with two kinds of backbone, namely Yolov8n and Yolov8m. The results demonstrate the superior performance of our approach in improving detection accuracy and robustness.

Index Terms—Head detection, auxiliary learning, LSTM, noise calibration, Yolov8

I. INTRODUCTION

Object detection has become a hot topic in computer vision tasks, which involves detecting instances of certain types of visual objects (e.g., humans, animals, or cars) in digital images [1]. Human head detection is one of the key problems in public safety scene understanding. Its goal is to estimate the distribution information of pedestrians in the scene, which plays an important role in risk perception and early warning, traffic control and scene statistical analysis. If pedestrian distribution statistics can be shown in real-time, the staff can be more targeted for statistical analysis, order maintenance and dangerous prevention [2].

Due to scene complexity, large-scale variance, and high crowd density in the real world, head detection remains a

challenging problem even though detection models have made considerable strides in recent years. Among many affecting factors, large-scale transformations and changes in the number of targets due to drastic variations of the scenes have a deleterious effect on the performance of the detection models. To tackle the problem of scene variations, many researchers try to take advantage of multi-scale features generated in deep convolutional neural networks at different levels [3], [4]. Feature pyramid network (FPN) is the typical architecture for multi-scale feature fusion. However, its performance suffers noticeably when detecting dense and small objects. To address these issues, we attempt to enhance the detector’s perception of the human head by introducing feature fusion through auxiliary learning.

Since the excellent detection performance of Yolov8, we make it as our baseline model. Our auxiliary learning method concentrates after the Neck part and introduces a heatmap prediction task that treats human head as positive class and the other areas as negative class. The heatmap prediction task is responsible for estimating the locations of the object centers. The response value in the heatmap is expected to be 1 when it locates in the center of the ground-truth object and the value gradually decreases exponentially as the distance between the heatmap location and the object center increases. The largest feature map is shared by the Yolov8 main task and the auxiliary learning task. Therefore, an additional reward from the auxiliary learning task can assist the main detection task to better perceive the position and size of the center of the human head. Consequently, models that incorporate an auxiliary learning task are able to superior detection performance

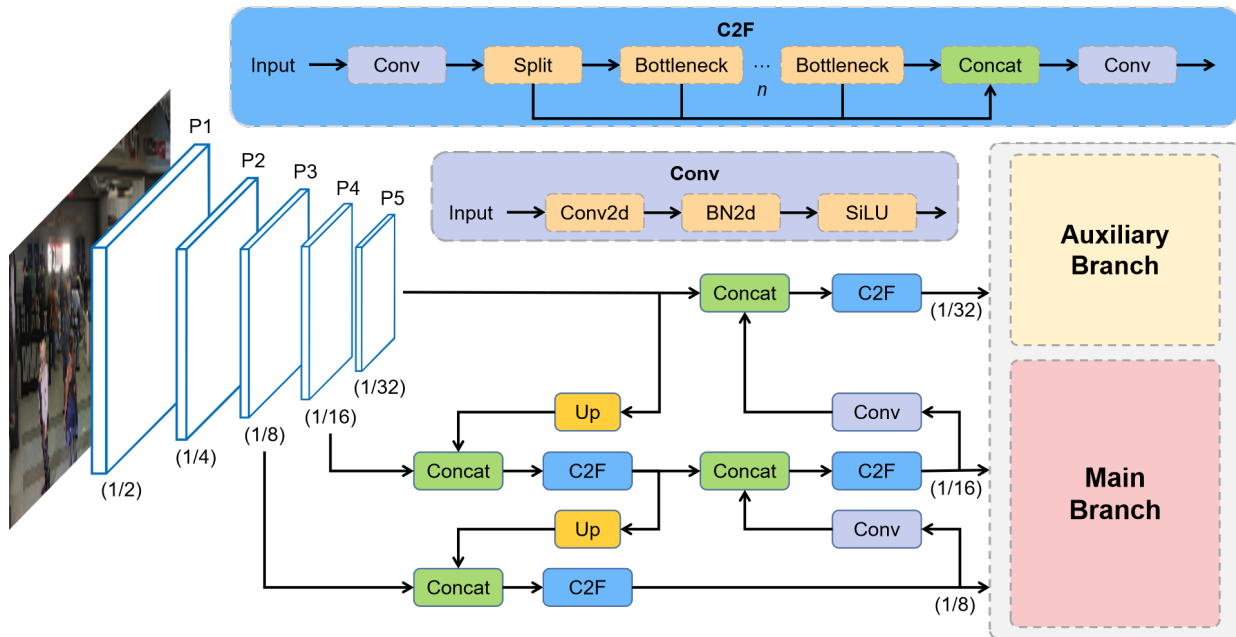


Fig. 1. Overview of our proposed network based on Yolov8. It contains two branches which share the feature map from the Neck. We construct the ALFF module in Auxiliary branch. NC-DFL is employed as the optimization function in the main branch.

compared to models that lack this task. In order to make full use of the features from main branch and conduct feature fusion, long short-term memory (LSTM) [5] is employed as a bridge between convolutional blocks. By leveraging the dependencies among the features, LSTM effectively filters out redundant information. Furthermore, the framework employs our proposed Noisy Calibration Distribution Focal Loss (NC-DFL) to promote model fitting and improve the accuracy and robustness of detection.

II. RELATED WORK

A. Head Detection

Head detection methods can be categorized into traditional methods and deep learning methods. The traditional methods work by using handcrafted features [6], [7], which suffers from limitations due to poor ability to generalise about the overall or local appearance of a person. With the advancements in deep learning, an increasing number of researchers are focusing their efforts on head detection [8]–[10]. Currently, there are two types of deep learning-based object detection: one-stage detection and two-stage detection. The most representative two-stage detection method is Region-CNN (RCNN) [11]. Many different RCNN variations, including Faster RCNN [12] and Mask RCNN [13], have been used to count crowds in recent years. The efficiency of one-stage detectors is significantly higher but the accuracy is lower because they directly predict the bounding box of targets without region proposal. [14] proposes Yolo network, which utilizes DarkNet as the feature extraction method. This allows Yolo to perform end-to-end optimization training, enabling it to simultaneously predict object bounding box locations and

category probabilities. Since then many excellent one-stage detection models have been proposed, such as RetinaNet [15], CenterNet [16] and FCOS [17].

B. Auxiliary Learning

Auxiliary learning is a technique that enhances the generalization ability of a primary task to handle unseen data, through training the primary task alongside auxiliary tasks [18]. By sharing features across these tasks, the model acquires relevant features that would not have been learned if it had only been trained on the main task. This broader support of features improves generalization to the main task even in the case of different interpretations of the input data. While similar to multi-task learning [19], auxiliary learning differs in that the primary task is performed with priority, while the auxiliary task is designed to assist the primary task. Auxiliary learning has demonstrated promising results in various domains, such as reinforcement learning [20], visual localization [21], and Instrument Segmentation [22]. To our knowledge, we are the first to apply auxiliary learning to head detection.

III. METHODOLOGY

In this paper, Our approach reinforces the target perception capability of Yolov8 by introducing Auxiliary Learning Feature Fusion (ALFF). The overview network can be referred to in Figure 1. Besides, we also introduce NC-DFL which facilitates model parameter fitting.

A. Network Architecture

In Figure 1, the input of Yolov8 object detection network is 640x640 images and the backbone network and Neck are generally the same as the previous version. Based on the

scaling factor, different size models of N/S/M/L/X scales are provided to meet different scenario requirements. To enrich the gradient flow, Yolov8 replaces the previous C3 module with the C2f module and adjusts the number of channels for different scale models. We introduce the auxiliary branch at the Head of Yolov8 so as to make full use of its excellent feature extraction capability.

B. Auxiliary Learning Feature Fusion

1) *Auxiliary Learning Task*: To detect multi-scale targets, Yolov8’s Neck outputs features in three sizes including 1/8, 1/16 and 1/32. Since the feature map of size 1/8 preserves the most information among the output features, we shall use it as a shared representative for the main and auxiliary task. In the lower part of Figure 2, the detection head of Yolov8 is replaced with the prevailing decoupled head construct, which separates the classification and detection heads. In addition, anchor-based is converted to anchor-free in order to enhance detection efficiency and accuracy. Therefore, encouraged by [16] which predicts the heatmap to estimate the location of targets, we set the auxiliary task as the prediction of human head heatmap. The auxiliary task is also responsible for estimating the locations of the object centers along with the main task, which can help the model better perceive the feature of targets.

For each bounding box $b^i = (c_x^i, c_y^i, w^i, h^i)$ in ground truth, the center of i th object is computed as $(c_x^i, c_y^i) = (\frac{x_1^i + x_2^i}{2}, \frac{y_1^i + y_2^i}{2})$ which will vary according to the size of the image scaling. Then, the heatmap response in (x, y) can be defined as:

$$p_{xy} = \sum_{i=1}^N \exp^{-[(x-c_x^i)^2 + (y-c_y^i)^2]/2\sigma^2} \quad (1)$$

where N denotes the number of objects in the image and σ represents the standard deviation. The scope of heatmap response is a circle of radius $\min(w^i, h^i)$.

2) *Feature Fusion with LSTM*: As mentioned above, 1/8 scaling feature map contains abundant scale-relevant information. Subsequently, the ALFF is employed to enhance the features for more precise estimation. ALFF consists of an LSTM and three sequential convolutional blocks that serve as a feature refiner. The architecture of each convolutional block is shown in the *Conv* of Figure 1.

LSTM has been widely utilized in information processing tasks such as video processing and data systems. Its exceptional capability to capture long-term dependencies is essential. When it comes to image processing, a series of convolutional layers are typically employed to process features in a step-by-step manner. During this process, features exhibit similarity, correlation, and refinement, leading to strong dependencies between features at each level. Referring to the utility of LSTM in crowd counting [23], we introduce LSTM into heatmap estimation as a information filter and dependency capturer. By leveraging the information from previous features, LSTM effectively filters the present feature. In an LSTM

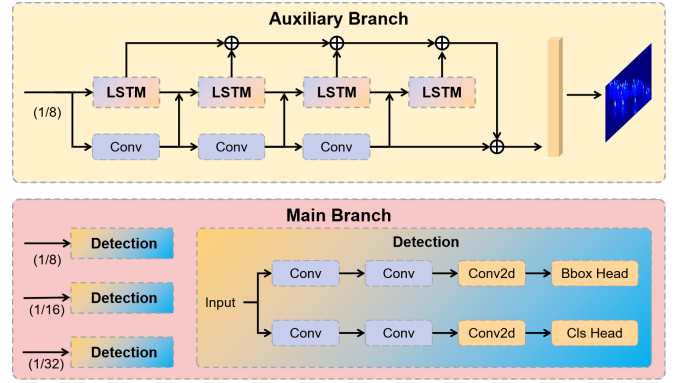


Fig. 2. Branches of the modified Yolov8. The upper part is our proposed Auxiliary Learning Feature Fusion (ALFF) Module which utilizes LSTM and convolutional blocks for further feature refinement. Feature map of auxiliary branch (1/8) is shared with main branch.

module, each layer computes the input sequence with the following function:

$$\begin{aligned} i_t &= \sigma(W_{ii}x_t + b_{ii} + W_{hi}h_{t-1} + b_{hi}) \\ f_t &= \sigma(W_{if}x_t + b_{if} + W_{hf}h_{t-1} + b_{hf}) \\ g_t &= \tanh(W_{ig}x_t + b_{ig} + W_{hg}h_{t-1} + b_{hg}) \\ o_t &= \sigma(W_{io}x_t + b_{io} + W_{ho}h_{t-1} + b_{ho}) \\ c_t &= f_t \odot c_{t-1} + i_t \odot g_t \\ h_t &= o_t \odot \tanh(c_t) \end{aligned} \quad (2)$$

where i_t, f_t, g_t, o_t are the input, forget, cell, and output gates, respectively. h_t is the hidden state at time t , c_t is the cell state at time t , x_t is the input at time t , and h_{t-1} is the hidden state of the layer at time $t-1$ or the initial hidden state at time 0. σ is the sigmoid function, and \odot is the Hadamard product. W_p and b_p denote the weight matrix and the bias term of the gate p .

In ALFF, the LSTM connects sequential features by making features as multi-node inputs and thus, which takes full advantage of the dependencies between hierarchical features for fusion. The LSTM is designed to use dependencies and filter hierarchical features. It employs input, memory, forget, and output gates to control the transmission state. The transmission state decides the filtering of the input feature, enabling the LSTM cell to produce the output that preserves valuable information while filtering out redundancy. Additionally, information from the current LSTM cell is passed on to the following cell, assisting it in filtering the subsequent input feature. By effectively concatenating the LSTM outputs, the information on hierarchical features can be well preserved. At the end of the auxiliary branch, a fully connected layer is used to modify the number of channels, followed by an upsampling layer that adjusts the feature map to the original size of the input.

C. Noisy Calibration Distribution Focal Loss

There are significant differences in scene and target distributions between the different datasets of head detection. When the number of targets increases or the scene changes drastically, it is difficult for the model to predict the location

and size of the targets accurately. We aim to modulate bounding box loss function to produce a stable and robust training procedure for the predictor to handle different datasets. The bounding box loss function utilized by Yolov8 is Distribution Focal Loss [24] which can be described as:

$$\text{DFL}(P_i, P_{i+1}) = -((y_{i+1} - y) \log(P_i) + (y - y_i) \log(P_{i+1})) \quad (3)$$

where y_i and y_{i+1} is explicitly enlarged probability (the nearest two to y). P_i is short for $P(y_i)$ which is the probability distribution of y_i .

When the output probabilities closely align with the desired outcome, it can be defined as individual saturation. However, early saturation will limit the optimizer to move. As the number of saturated individuals increases, it is more likely to converge to a local minima, leading to overfitting eventually [25]. To mitigate this, it is beneficial to appropriately delay sample saturation to promote global convergence in regular experiments. For datasets with simple scenarios and fewer targets, the above procedure is effective. However, achieving convergence is particularly challenging when the scene is complex and the number of targets is large. During the training stage, the detection model remains underfitted for most samples. To address this, we adopt an opposite perspective and promote sample saturation. By increasing the logit value of underfitted samples, we enhance their contribution during back-propagation. This adjustment provides the optimizer with more opportunities to progress toward global convergence. To calibrate the logit values, we utilize Gaussian noise as a carrier, effectively aiding model fitting. Therefore, the logits fed into noise calibration can be rewritten as:

$$y^G = y[1 + \alpha \cdot (\mu + \sigma |\xi|)] \quad (4)$$

where μ and σ are the mean and the standard variance of the Gaussian noise. $\xi \sim \mathcal{N}(0,1)$. hyper-parameter α is used to adjust the scale of noise. Here, we set the mean value to 0. Therefore, the model can adjust the logits and get better global convergence. Gaussian noise can further improve the robustness of training effectively.

In contrast, our NC-DFL can be calibrated for a simple training set as follows

$$y^G = y[1 - \alpha \cdot (\mu + \sigma |\xi|)] \quad (5)$$

We hereby obtain our noisy calibration distribution focal loss (NC-DFL):

$$\text{DFL}(P_i, P_{i+1})^G = -((y_{i+1}^G - y^G) \log(P_i^G) + (y^G - y_i^G) \log(P_{i+1}^G)), \quad (6)$$

$$y^G = y[1 \pm \alpha \cdot (\mu + \sigma |\xi|)]$$

IV. EXPERIMENTS

A. Datasets and Settings

We evaluate our proposed method on two public datasets. The detection results of both datasets are visualized in Figure 3.

TABLE I
SNECE DISTRIBUTION OF GTA_L AND GTA_H DATASETS IN GTA_HEAD.

Density	Training Set		Testing Set	
	Snece	Number/Image	Snece	Number/Image
Low Density	7	77.30		
	9	93.97	33	34.69
	17	41.95	34	41.99
	19	76.73	35	28.25
	20	39.25		
High Density	3	256.68		
	4	224.31		
	5	284.10	22	228.01
	8	105.99	24	127.11
	11	235.22	27	159.01
	12	185.99	29	216.69
	13	195.80		
	21	286.26		

SCUT-HEAD: SCUT-HEAD [3] is a publicly large-scale head detection dataset, including 4405 frames labeled with 111251 bounding boxes. There are two parts in this dataset. The first part consists of 2,000 images extracted from classroom surveillance video. The other part consists of 2,405 images captured from the Internet.

GTA_Head: GTA_Head [26] is a large-scale virtual world dataset for head detection, including 5096 images labeled with 1732043 bounding boxes. It contains numerous complex scenes: stadiums, indoor shopping malls, subways and squares, etc. To assess our framework under different pedestrian densities, we select scenes according to the density and divide them into GTA_L and GTA_H based on the average number of person. Those scenes with density of less than 100 per frame are covered in GTA_L which consists of a total of 8 scenarios, with 5 scenarios in the training set and 3 scenarios in the testing set. The GTA_H comprises 8 scenes in the training set and 4 scenes in the testing set and the density greater than 100 less than 300. The scene distribution of GTA_L and GTA_H can be found in Table I.

B. Implementation details

There are different variants with distinct network architectures in Yolov8. Considering the requirements of high accuracy and speed for the head detection task, we adopt Yolov8n and Yolov8m pretrained on COCO as our representative baseline models. In the following experiments, all methods are implemented using the Python Pytorch framework on an NVIDIA RTX 3090Ti GPU. The batch size is set to 16 for 50 epochs. We adopt the initial learning rate 1×10^{-2} with the weight decay of 5×10^{-4} . Based on our pre-training results, we find that α in Equation 6 works best when it is 1.0, which will be maintained in subsequent experiments.

C. Results and Discussion

1) *Evaluation on SCUT-HEAD:* Table II shows the quantitative experimental result of SCUT-HEAD dataset. Overall our modified Yolov8 achieved excellent performance and significantly outperforms other classical detectors in all evaluation

TABLE II
THE DETECTION RESULTS OF THE PROPOSED METHOD WITH OTHER CLASSICAL METHODS ON SCUT-HEAD DATASETS.

Approach	Backbone	SCUT-HEAD_PartA			SCUT-HEAD_PartB		
		AP50	AP75	AP50-95	AP50	AP75	AP50-95
RetinaNet [15]	R50-FPN	0.904	0.203	0.386	0.868	0.512	0.489
CenterNet [16]	R50-FPN	0.949	0.414	0.476	0.937	0.573	0.54
FCOS [17]	R101-FPN	0.927	0.405	0.471	0.898	0.487	0.456
Foveabox [27]	R101	0.9	0.194	0.377	0.894	0.485	0.482
Yolov8	YOLOv5n	0.9503	0.2837	0.4371	0.9492	0.6027	0.5561
Yolov8(Ours)	YOLOv5n	0.95	0.2958	0.441	0.9496	0.6053	0.558
Yolov8	YOLOv5m	0.9703	0.332	0.4666	0.9624	0.6285	0.5750
Yolov8(Ours)	YOLOv5m	0.9715	0.3682	0.4808	0.9633	0.6299	0.5752

TABLE III
THE DETECTION RESULTS OF THE PROPOSED METHOD WITH OTHER CLASSICAL METHODS ON GTA_L AND GTA_H DATASETS.

Approach	Backbone	GTA_L			GTA_H		
		AP50	AP75	AP50-95	AP50	AP75	AP50-95
RetinaNet [15]	R50-FPN	0.513	0.029	0.127	0.293	0.066	0.78
CenterNet [16]	R50-FPN	0.555	0.019	0.144	0.301	0.075	0.119
FCOS [17]	R101-FPN	0.462	0.011	0.107	0.477	0.126	0.135
Foveabox [27]	R101	0.521	0.023	0.126	0.439	0.101	0.125
Yolov8	YOLOv5n	0.5654	0.03641	0.1616	0.4843	0.1527	0.2121
Yolov8(Ours)	YOLOv5n	0.5725	0.0381	0.1686	0.4849	0.1512	0.2104
Yolov8	YOLOv5m	0.6661	0.09988	0.2133	0.5824	0.2143	0.2696
Yolov8(Ours)	YOLOv5m	0.6907	0.1121	0.2394	0.591	0.2292	0.2808

metrics. As mentioned in Section 3, the introduction of the anchor-free prediction of human head heatmap auxiliary task aids the model in better perceiving the features of the targets. Consequently, both Yolov8 models are enhanced through our approach. Specifically, the modified Yolov8m performs best among all baselines with AP50 scores of 0.9715 and 0.9633 on two parts. Besides, for stricter metrics, our approach gives a 2.2%-10.9% improvement on AP75 and a 0.03%-2.95% improvement on AP50-95 for Yolov8 on both backbones.

2) *Evaluation on GTA_Head*: The GTA_L and GTA_H datasets are more challenging because of the complex scenes and scale variations. Table III shows the quantitative experimental result. Yolov8m is also the best-performing detector, and our improvement method helps Yolov8m further improve the full range of evaluation metrics. More significant AP75 enhancement, with 12.23% in GTA_L and 6.95% in GTA_H. As evident from this, our improved Yolov8 utilizes the advanced model architecture of Yolov8, which not only performs well in simple scenes but also significantly enhances the accuracy of head detection in complex and high-density datasets. Moreover, our framework improves the perceptual capability of YOLOv8 while enhancing the robustness of the model across different scenes and target distributions. Due to the diverse nature of the GTA_Head dataset, the detection performance of the original YOLOv8 decreases. Our NC-DFL method satisfactorily addresses this issue, achieving AP50 of 0.6907 in low-density scenarios and 0.591 in high-density scenarios within the GTA_Head dataset. The superior performance of the modified Yolov8 in this challenging scenario further reflects

the excellent universality and power of our method.



Fig. 3. From top to bottom are examples from SCUT-HEAD PartA, SCUT-HEAD PartB, GTA_L and GTA_H.

3) *Ablation Studies*: We make ablation study to assess the effects of removing ALFF and NC-DFL, respectively. For ablation dataset, we select the GTA_H which presents the most challenging task. Experimental results in Table IV conducted on the GTA_H dataset reveal that in the absence of NC-DFL, our auxiliary branch with the LSTM network can improve the performance of head detection to some extent. Additionally,

TABLE IV

ABLATION STUDY OF OUR FRAMEWORK ON THE GTA_H DATASET. ALFF AND NC-DLF DENOTE AUXILIARY BRANCH AND NOISY CALIBRATION DISTRIBUTION FOCAL LOSS. WE REMOVE THE ABOVE COMPONENTS ONE BY ONE AND OBSERVE THE DETECTION PERFORMANCE.

ALFF	NC-DLF	GTA_H		
		AP50	AP75	AP50-95
×	×	0.5824	0.2143	0.2696
✓	×	0.5866	0.2384	0.2802
×	✓	0.5879	0.219	0.2742
✓	✓	0.591	0.2292	0.2808

the standalone introduction of NC-DLF significantly enhances the performance of complex tasks. However, compared with our final results, we can observe the performance degradation of individual components. These observations indicate that ALFF and NC-DLF positively contribute to achieving the best results.

V. CONCLUSION

In this paper, we propose a modified Yolov8 that enhances head detection performance by reinforcing target perception. To aid the model in perceiving targets, we introduce Auxiliary Learning Feature Fusion, which combines LSTM and convolutional blocks. This module provides additional information to enhance target understanding. Moreover, we leverage Noise Calibration in the Distribution Focal Loss to facilitate model fitting and improve the detection accuracy. Experimental results show the superior performance of our approach in Yolov8n and Yolov8m, leading to improved detection accuracy and robustness. In summary, our modified Yolov8 approach enhances head detection performance by employing ALFF and NC-DLF. In future work, we will simplify the model while maintaining accuracy and try to use our modified Yolov8 for the detection of a wider variety of targets.

VI. ACKNOWLEDGMENT

This work was supported in part by Grants of National Key R&D Program of China 2020AAA0108300, the Shenzhen University 2035 Program for Excellent Research 00000224 and the National Nature Science Foundation of China under Grant 62171288.

REFERENCES

- [1] Zhengxia Zou, Keyan Chen, Zhenwei Shi, Yuhong Guo, and Jieping Ye. Object detection in 20 years: A survey. *Proceedings of the IEEE*, 2023.
- [2] Gaurav Tripathi, Kuldeep Singh, and Dinesh Kumar Vishwakarma. Convolutional neural networks for crowd behaviour analysis: a survey. *The Visual Computer*, 35:753–776, 2019.
- [3] Dezhi Peng, Zikai Sun, Zirong Chen, Zirui Cai, Lele Xie, and Lianwen Jin. Detecting heads using feature refine net and cascaded multi-scale architecture. In *2018 24th International Conference on Pattern Recognition (ICPR)*, pages 2528–2533. IEEE, 2018.
- [4] Ross Girshick. Fast r-cnn. In *Proceedings of the IEEE international conference on computer vision*, pages 1440–1448, 2015.
- [5] Sepp Hochreiter and Jürgen Schmidhuber. Long short-term memory. *Neural computation*, 9(8):1735–1780, 1997.
- [6] Markus Enzweiler and Dariu M Gavrila. Monocular pedestrian detection: Survey and experiments. *IEEE transactions on pattern analysis and machine intelligence*, 31(12):2179–2195, 2008.
- [7] Zhe Lin and Larry S Davis. Shape-based human detection and segmentation via hierarchical part-template matching. *IEEE transactions on pattern analysis and machine intelligence*, 32(4):604–618, 2010.
- [8] Jing Han, Xiaoying Wang, Xichang Wang, and Xueqiang Lv. Cfnct: Head detection network based on multi-layer feature fusion and attention mechanism. *IET Image Processing*, 17(7):2032–2042, 2023.
- [9] Junwen Liu, Yongjun Zhang, Jianbin Xie, Yan Wei, Zewei Wang, and Mengjia Niu. Head detection based on dr feature extraction network and mixed dilated convolution module. *Electronics*, 10(13):1565, 2021.
- [10] Wei Li, Hongliang Li, Qingbo Wu, Fanman Meng, Linfeng Xu, and King Ngai Ngan. Headnet: An end-to-end adaptive relational network for head detection. *IEEE Transactions on Circuits and Systems for Video Technology*, 30(2):482–494, 2019.
- [11] Shifeng Zhang, Longyin Wen, Xiao Bian, Zhen Lei, and Stan Z Li. Occlusion-aware r-cnn: detecting pedestrians in a crowd. In *Proceedings of the European Conference on Computer Vision (ECCV)*, pages 637–653, 2018.
- [12] Shaoqing Ren, Kaiming He, Ross Girshick, and Jian Sun. Faster r-cnn: Towards real-time object detection with region proposal networks. *Advances in neural information processing systems*, 28, 2015.
- [13] Kaiming He, Georgia Gkioxari, Piotr Dollár, and Ross Girshick. Mask r-cnn. In *Proceedings of the IEEE international conference on computer vision*, pages 2961–2969, 2017.
- [14] Zixiao Zhang, Xiaoqiang Lu, Guojin Cao, Yuting Yang, Licheng Jiao, and Fang Liu. Vit-yolo: Transformer-based yolo for object detection. In *Proceedings of the IEEE/CVF international conference on computer vision*, pages 2799–2808, 2021.
- [15] Tsung-Yi Lin, Priya Goyal, Ross Girshick, Kaiming He, and Piotr Dollár. Focal loss for dense object detection. In *Proceedings of the IEEE international conference on computer vision*, pages 2980–2988, 2017.
- [16] Xingyi Zhou, Dequan Wang, and Philipp Krähenbühl. Objects as points. *arXiv preprint arXiv:1904.07850*, 2019.
- [17] Zhi Tian, Chunhua Shen, Hao Chen, and Tong He. Fcos: Fully convolutional one-stage object detection. In *Proceedings of the IEEE/CVF international conference on computer vision*, pages 9627–9636, 2019.
- [18] Shikun Liu, Andrew Davison, and Edward Johns. Self-supervised generalisation with meta auxiliary learning. *Advances in Neural Information Processing Systems*, 32, 2019.
- [19] Rich Caruana. Multitask learning. *Machine learning*, 28:41–75, 1997.
- [20] Max Jaderberg, Volodymyr Mnih, Wojciech Marian Czarnecki, Tom Schaul, Joel Z Leibo, David Silver, and Koray Kavukcuoglu. Reinforcement learning with unsupervised auxiliary tasks. *arXiv preprint arXiv:1611.05397*, 2016.
- [21] Abhinav Valada, Noha Radwan, and Wolfram Burgard. Deep auxiliary learning for visual localization and odometry. In *2018 IEEE international conference on robotics and automation (ICRA)*, pages 6939–6946. IEEE, 2018.
- [22] Mobarakol Islam, Daniel Anojan Atputharuban, Ravikiran Ramesh, and Hongliang Ren. Real-time instrument segmentation in robotic surgery using auxiliary supervised deep adversarial learning. *IEEE Robotics and Automation Letters*, 4(2):2188–2195, 2019.
- [23] Di Wu, Zheyi Fan, and Shuhan Yi. Crowd counting based on multi-level multi-scale feature. *Applied Intelligence*, pages 1–11, 2023.
- [24] Xiang Li, Chengqi Lv, Wenhui Wang, Gang Li, Lingfeng Yang, and Jian Yang. Generalized focal loss: Towards efficient representation learning for dense object detection. *IEEE transactions on pattern analysis and machine intelligence*, 45(3):3139–3153, 2022.
- [25] Binghui Chen, Weihong Deng, and Junping Du. Noisy softmax: Improving the generalization ability of dcnn via postponing the early softmax saturation. In *Proceedings of the IEEE conference on computer vision and pattern recognition*, pages 5372–5381, 2017.
- [26] Xiaopin Zhong, Guankun Wang, Weixiang Liua, Zongze Wua, and Yuanlong Deng. Mask focal loss for dense crowd counting with canonical object detection networks. *arXiv preprint arXiv:2212.11542*, 2022.
- [27] Tao Kong, Fuchun Sun, Huaping Liu, Yuning Jiang, Lei Li, and Jianbo Shi. Foveabox: Beyond anchor-based object detection. *IEEE Transactions on Image Processing*, 29:7389–7398, 2020.